PAPER REFERENCE: *A-VI.3*

MICROMAGNETIC SIMULATIONS OF MAGNETIZATION IN CIRCULAR COBALT DOTS

L. D. Buda*, I. L. Prejbeanu, U. Ebels and K. Ounadjela

IPCMS (CNRS-ULP), 23 rue du Loess 67037 Strasbourg Cedex, France

Abstract

Using tri-dimensional micromagnetic simulations, the phase diagram including different magnetic ground states is computed for circular Co dots as a function of the dot dimensions. The presence of a large perpendicular magnetocrystalline anisotropy induces a shift of the boundary between the ground states and increases the number of possible stable states.

Keywords: micromagnetics, circular Co dots

* Corresponding Author: Tel. +33 388107077; Fax. +33 388107249; E_mail: Liliana.Buda@ipcms.u-strasbg.fr

1. Introduction

Over the past decade, magnetic materials structured on the submicron length scale have been the subject of increasing interest because of their possible applications as high-density storage media [1]. Therefore the magnetisation configurations as well as the corresponding reversal processes are of a primary concern. The magnetic properties of small elements are controlled by their shape, dimensions and material parameters. In this context, regular arrays of submicron dots of different geometries, such as rectangles, squares, triangles, circles, rings or pentagons were fabricated using materials like Permalloy, Co or Fe [2].

The understanding of the magnetic properties of such nanoelements requests a rigorous analysis, using experimental studies correlated with numerical simulations. Experimental techniques, such as the magneto-optical Kerr effect magnetometry or magnetic force microscopy (MFM) either enable us to extract information on the average magnetisation or give limited access to the spatial variation of the magnetisation. Additional information of the fine details of the internal distribution of the magnetisation can be obtained only by micromagnetic modelling.

In this paper, a systematic investigation of the ground state configurations in circular Co dots is carried out by means of 3D micromagnetic calculations. The first part describes the numerical tools used and in the second part the numerical results are discussed.

2. Computational details

According to micromagnetic theory [3], a ferromagnetic system consisting of a large number of individual magnetic spins is described using continuous functions for the magnetisation, the

fields and the energies. Moreover the amplitude of the magnetisation vector $\vec{M}(\vec{r})$ has to be constant $\left|\vec{M}(\vec{r})\right| = M_s \left|\vec{m}(\vec{r})\right| = M_s$ but its orientation may change from one position to another. In this approach, for a given magnetisation distribution $\vec{M}(\vec{r})$ the Gibbs free energy is:

$$G(\vec{M}) = \int_{Volum} dV \left[A_{ex} (\nabla \vec{m})^2 + g(\vec{m}, \vec{u}_k) - \frac{1}{2} \mu_o M_s (\vec{m} \cdot \vec{H}_{dem}) - \mu_o M_s (\vec{m} \cdot \vec{H}_{app}) \right]$$

where $\vec{H}_{app}$ is the applied field, A_{ex} is the exchange constant and $\vec{H}_{dem}$ is the demagnetising field. The magnetocrystalline anisotropy energy density g for a uniaxial crystal $\vec{u}_k$ is given by $g(\vec{m}, \vec{u}_k) = K_u [1 - (\vec{m} \cdot \vec{u}_k)^2]$, where K_u is the anisotropy constant. Using the variational principle to minimise the Gibbs free energy with respect to the magnetisation $\vec{M}$, the equation of the stable equilibrium state reads $\vec{m} \times \vec{H}_{eff} = 0$, where the effective field $\vec{H}_{eff}$ is defined as $\vec{H}_{eff} = -\delta G / \delta \vec{M}$. Because the magnetostatic interaction is of long-range, the micromagnetic equation is highly non-linear and analytical solutions can only be found for very special cases [4]. For systems having a complex geometry, numerical simulations are requested. To this purpose several numerical approaches were proposed using either the finite element method [5,6] or the finite difference method [7]. For the simulations reported here, a finite difference algorithm was developed based on the time integration of the Landau-Lifshitz–Gilbert equation (LLG):

$$(1 + \alpha^2) \frac{\partial \vec{M}}{\partial t} = -\gamma (\vec{M} \times \mu_0 \vec{H}_{eff}) - \frac{\alpha \gamma}{M_s} \vec{M} \times (\vec{M} \times \mu_0 \vec{H}_{eff})$$

Here γ is the gyromagnetic ratio of the free electron spin and α is the damping parameter. The ferromagnetic system is spatially divided into $N_x \times N_y \times N_z$ tetragonal cells and within each cell the magnetisation is assumed to be uniform. In order to assure a good description of the magnetisation details for example inside a domain wall or a vortex, the size of the mesh has to be smaller than the characteristic lengths of the material: the exchange length $l_{ex} = \sqrt{A_{ex} / \left(\mu_0 M_s^2\right)}$ and the Bloch wall parameter $\Delta_0 = \sqrt{A_{ex} / K_u}$. The most intensive part of the computation procedure in micromagnetic simulations is the evaluation of the demagnetising field. In our case the stray field is evaluated from the magnetostatic interaction energy between two mesh cells [8]. For a regular mesh the Fast Fourier Transform (FFT) implementation reduces the computation time considerably. Starting from a given magnetisation distribution, the integration of the LLG equation using an implicit Crank-Nicholson method provides the evolution of the magnetisation in time towards the equilibrium state. The equilibrium is reached if the maximum value of the torque decreases below a given tolerance, with $\left|\vec{m} \times \vec{H}_{eff}\right| \leq 10^{-6} M_s$. Because we are interested only in the static configuration and not in the intermediate states a large value for the damping parameter $\alpha = 1$ is used in order to accelerate the computation.

In the present study, the described procedure was applied to a circular geometry. The choice of the discretization scheme is validated by the fact that the numerical 'roughness' (generated by the square mesh representation) corresponds to the real imperfections on the lateral dot surface, arising for example from the resolution of the patterning methods used.

3. Ground states of circular Co dots

The magnetic stable states exhibited by a circular dot depend on the element size (diameter and thickness), the intrinsic material parameters (spontaneous magnetisation, crystal anisotropy) and the magnetic history (remnant or demagnetised state, field orientation). MFM measurements performed on circular Co(0001) dots [9] clearly showed two magnetic contrasts: a strong black–white dipolar contrast arising from an in-plane single domain configuration and a weak contrast associated with a flux closure configuration (vortex-like state). Furthermore an irreversible transition could be induced from the single domain state to the vortex state by the MFM tip stray field, indicating that the vortex state is the energetically lower state for the investigated dimensions.

In order to explore the evolution of these two states as a function of the dot diameter (ϕ) and the thickness (t), micromagnetic simulations were carried using the material parameters of Co, with $M_s = 1.4\times10^6\, A/m$, $A_{ex} = 1.4\times10^{-11}\, J/m$, $K_u = 5.0\times10^5\, J/m^3$. Starting either from an in-plane or an out-of-plane saturated state the system relaxes to an in-plane single domain (SD) or to a vortex-like state (V) (Fig. 1a). The state having the lowest energy value represents the ground state of the system.

In the vortex state the magnetisation curls in a circular path along the dot border leading to a singularity (vortex) in the dot centre where the magnetisation turns out of plane (OZ direction). In order to properly represent such a magnetic singularity involving a rapid variation of the magnetisation, the mesh size needs to be chosen sufficiently small. As shown in figure 1b for the M_z component of the vortex state, the vortex is not obtained, if the mesh size is larger than $2l_{ex}$. For the results reported here a mesh size of 0.75 l_{ex} ($l_{ex} = 3.37$ nm, $\Delta_0 = 5.28$ nm) was used providing an accurate description of the vortex structure.

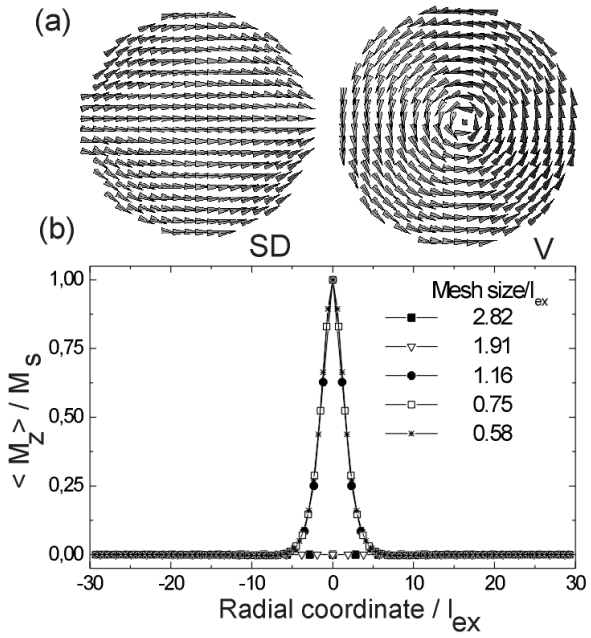

Fig. 1. (a) The magnetisation vector plot for the single domain (SD) and vortex-like (V) state. (b) The out-of-plane magnetisation profile along a radial section of the V state in a dot of ϕ = 200 nm/ t = 2 .5 nm as a function of the discretization mesh.

First, Co dots with zero magnetocrystalline anisotropy ($K_u = 0\ J/m$) are discussed. The different ground state configurations in zero applied field of such polycrystalline Co dots are summarised in figure 2. The critical diameter at which the in-plane single domain state renders the vortex state energetically more favourable decreases with increasing thickness. For these two possible ground states the total energy arises from the demagnetisation and the exchange contribution. For the in-plane single domain state the magnetisation lies in the dot plane being almost uniform. The energy of this state is dominated by the magnetostatic contribution because of the magnetic charges induced on the lateral surface of the dot. In contrast, for the vortex like state the magnetic flux being closed, the magnetostatic energy is drastically reduced. But the central

region including the vortex core represents a large concentration of exchange energy which becomes comparable to the magnetostatic energy of a SD state if the dot diameter approaches the vortex core diameter. Since the magnetostatic energy of the in-plane SD increases with increasing dot thickness, the critical diameter of the boundary decreases with increasing *t*.

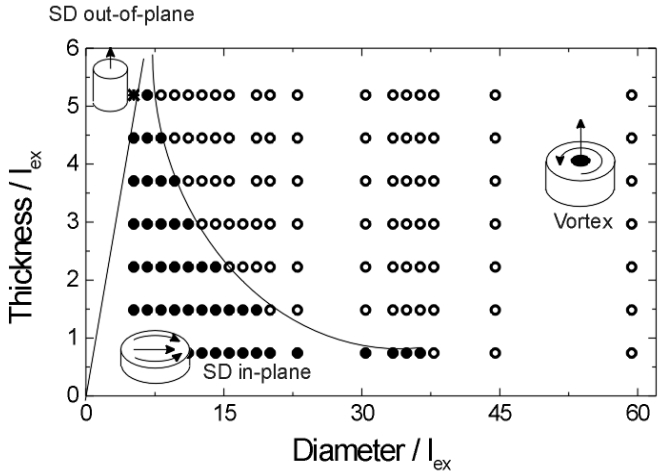

Fig. 2. The ground state phase diagram for polycrystalline ($K_u = 0\ J/m^3$) circular Co dots.

In addition to the in-plane single domain state and the vortex state, a third configuration is found corresponding to an out-of-plane single domain state when the thickness is comparable to or larger than the dot diameter. For this range of aspect ratios ($t \geq \phi$), the dot corresponds to an elongated wire and the shape anisotropy prefers an alignment of the magnetisation along the long wire axis.

A similar phase diagram has been reported by [10] and [2] for polycrystalline permalloy circular dots. In this case the boundary between the in-plane SD and the V state is shifted to much larger values of *t* and ϕ. This is explained by the fact that the saturation magnetisation of permalloy is smaller than the one of Co.

Including now a uniaxial magnetocrystalline anisotropy perpendicular to the dot plane a similar ground state phase diagram was computed for Co dots as shown in figure 3. It is noted that the anisotropy considered here is weaker than the demagnetisation energy yielding a Q factor $\left(Q = 2K_u / \mu_0 M_s^2\right)$ around 0.4 for Co. While the presence of such an anisotropy lowers the critical thickness of the boundary between the in-plane to the out-of-plane SD state (at constant diameter), it plays only a minor role for the in-plane SD to V transition. This difference is due to the relative volumes of perpendicular magnetisation in the out-of-plane SD state and the vortex state. For the latter this volume is small compared to the diameter and in consequence the boundary between the in-plane SD and V ground states is only slightly shifted towards smaller values of t and ϕ.

A strong influence of the perpendicular magnetocrystalline anisotropy (PMA) is exhibited for a dot thickness above 15-20 nm where a transition from the vortex state into a weak circular stripe domain state takes place. As shown in Fig. 4, the size of the central region where the magnetisation is pointing upwards has increased drastically to an almost domain like region. Already at t = 15 nm and 20 nm small oscillations of M_z across the radius set in, but the magnetisation is still predominantly in-plane. These oscillations have developed at t = 25 nm into a circular weak stripe structure, with a period which is about half the period of the oscillations at t = 20 nm. A similar concentric ring structure has been reported in [11] for 25 nm thick square Co dots. This thickness of t = 25 nm corresponds to the thickness range, where in continuous epitaxial Co(0001) films a reduction of the PMA energy is achieved by the formation of a weak stripe domain structure with the magnetisation canted out of the plane. The lateral confinement of this weak stripe structure induces a circular arrangement of the domains in order to reduce the in-plane demagnetisation field. A qualitative boundary between the continuous transition from the vortex state to the weak stripe state is indicated in figure 3 by the dotted line.

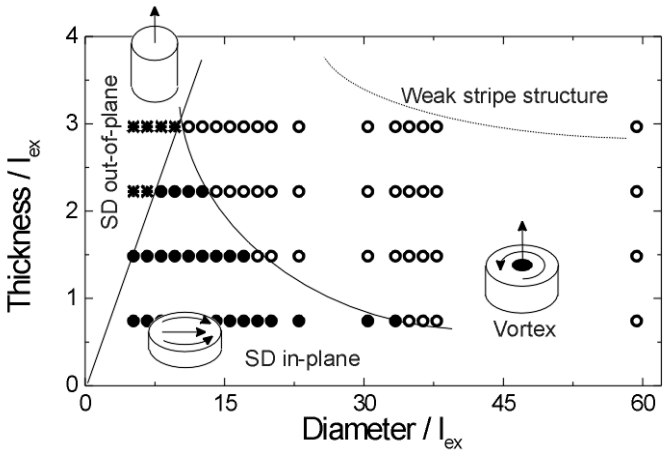

Fig. 3. The ground state phase diagram computed for epitaxial Co(0001) dots with $K_u = 5.0 \times 10^5 \ J/m^3$.

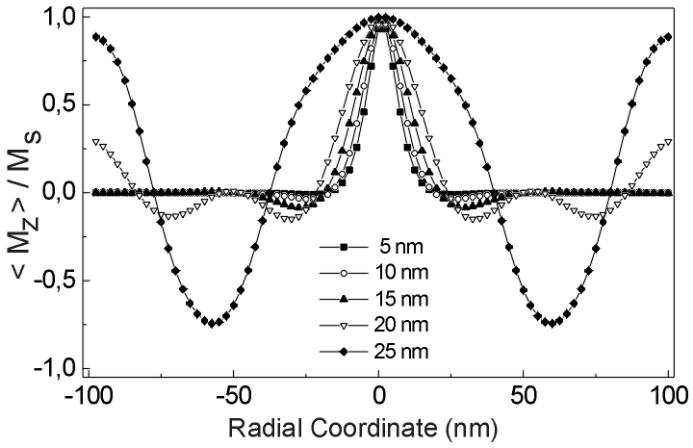

Fig. 4. The out-of-plane magnetisation line scan profiles across diameter as a function of dot thickness for ϕ = 200 nm and considering a large perpendicular magnetocrystalline anisotropy.

4. Summary

Using 3D micromagnetic simulations, the phase diagram of circular Co dots with and without perpendicular magnetocrystalline anisotropy has been calculated. While the anisotropy plays a minor role for the in-plane single domain to vortex transition, it shifts the boundary for the in-plane to out-of-plane single domain state and leads to a weak stripe structure for thickness above 15 nm.

Acknowledgements

The work was partially supported by EC Program 'NanoPTT' n° G5RD-CT-1999-00135 and EC Program 'Magnoise' n° IST-1999-11433.

References

[1] J. -G. Zhu, Y. Zheng, G. A. Prinz, J. Appl. Phys. 87, 2000, 6668.

[2] R. P. Cowburn , J. Phys. D: Appl. Phys.33, 2000, R1 and references therein.

[3] W. F. Brown Jr., Micromagnetics, Wiley, New York, 1963.

[4] A. Aharoni, Introduction to the Theory of Ferromagnetism, Clarendon Press, Oxford, 1997

[5] J. Fidler, T. Schrefl, J. Phys. D, Appl. Phys. 33, 2000, R135.

[6] D. R. Fredkin, T. R. Koehler, IEEE Trans. Magn. MAG-24, 1987, 3385.

[7] D. V. Berkov, K. Ramstöck, A. Hubert, Phys. Status Solidi A 137, 1993, 207.

[8] M. E. Schabes, A. Aharoni, IEEE Trans. Magn. MAG-23, 1987, 3882.

[9] M. Demand, M. Hehn, K. Ounadjela, R. L. Stamps, E. Cambril, A. Cornette, F. Rousseaux, J. Appl. Phys. 87, 2000, 5111.

[10] C. Miramond , C. Fermon, F. Rousseaux, D. Decanini, F. Carcenac, J. Magn. Magn. Mat. 165, 1997, 500

[11] M. Hehn, K. Ounadjela, J. P. Bucher, F. Rousseaux, D. Decanini, B. Bartenlian, C. Chappert, Science 272, 1996, 1782.